Supporting Information for

Breakdown of the Static Picture of Defect Energetics in Halide Perovskites: the Case of the Br Vacancy in $CsPbBr_3$

Ayala V. Cohen,[1] David A. Egger,[2,3] Andrew M. Rappe,[4] and Leeor Kronik[1]

[1] *Department of Materials and Interfaces, Weizmann Institute of Science, Rehovoth 76100, Israel.*

[2] *Institute of Theoretical Physics, University of Regensburg, 93040 Regensburg, Germany.*

[3] *Department of Physics, Technical University of Munich, 85748 Garching, Germany*

[4]*Department of Chemistry, University of Pennsylvania, Philadelphia, PA 19104–6323, USA.*

1. Comparison of PBE and HSE+SOC results

All calculations reported in the main text were performed using the PBE exchange-correlation functional, which is computationally efficient. However, it is known that more accurate results are obtained with the HSE[1] functional, in conjunction with spin-orbit coupling (SOC).[2] To ascertain that the trends obtained with PBE are indeed representative of those obtained at a higher level of theory, we considered five representative geometries with defect levels that span a range of fluctuations and performed additional calculations with the HSE functional, including spin-orbit coupling (SOC). The results are given in Table S1. Clearly, the trend is indeed maintained, with the spread of energies only growing for HSE+SOC. Therefore, our PBE calculations are sufficient for establishing the dynamic nature of the defect level.

Table S1: Comparison between selected defect level eigenvalues of the Br vacancy in $CsPbBr_3$ that span a range of fluctuations, taken from specific snapshots of the PBE-based MD calculation, to results obtained from HSE+SOC calculations for the same geometries. All eigenvalues are given with respect to the VBM taken as zero.

PBE defect eigenvalues [eV]	**HSE + SOC defect eigenvalues [eV]**
2.01	1.83
1.88	1.63
1.69	1.42
1.43	1.12
1.38	1.10

A similar procedure was performed for the GaAs supercell. Here we considered nineteen representative geometries, sampled from the MD run in intervals of three MD steps, and performed additional calculations with HSE+SOC for these geometries. The results are given in Fig. S1. Clearly, the trend is maintained here as well. Although the spread of the defect energies is larger compared to that obtained with PBE due to the opening of the band gap, it is still significantly smaller than the spread of the HaP defect energies.

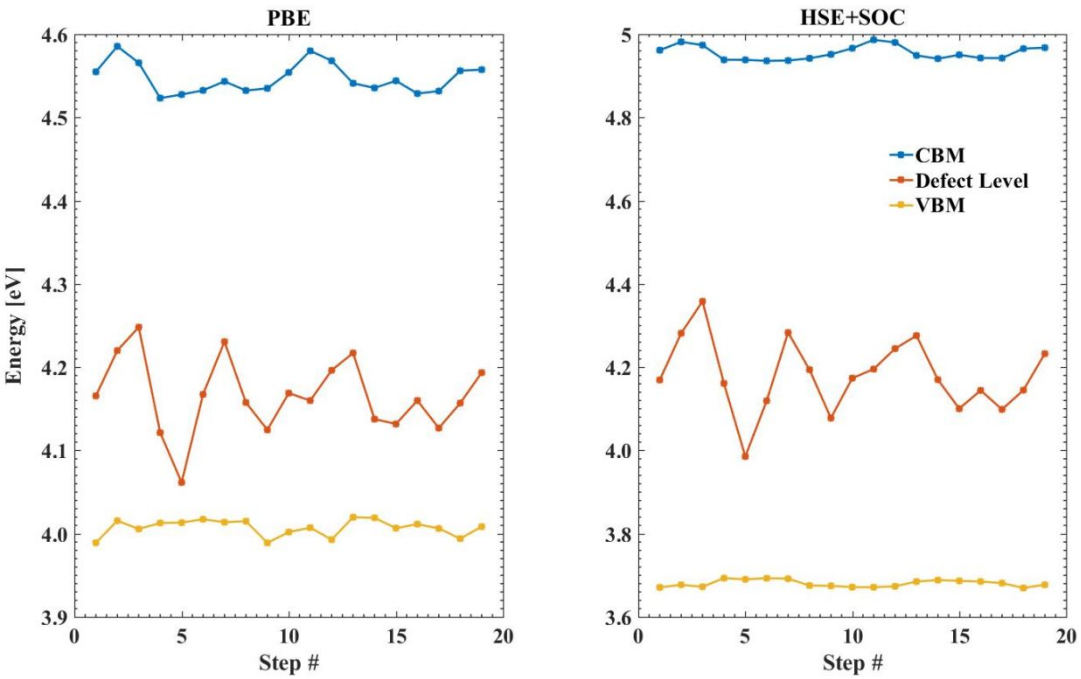

Figure S1: Comparison between selected VBM, defect level, and CBM eigenvalues of the As_{Ga} anti-site in GaAs that span a range of fluctuations, taken from the PBE-based MD calculation, to results obtained from HSE+SOC calculations for the same geometries.

2. Convergence of the MD time step

Unlike its more heavily studied counterpart, $MAPbI_3$, $CsPbBr_3$ does not require a particularly short time step to capture its behavior due to the lack of an organic molecule. This is clearly demonstrated in Fig. S2, where eigenvalues from the 10 fs MD run are compared to the eigenvalues received from an MD run with a 2 fs time step. Clearly, the 10 fs time step is sufficient for capturing the magnitude of the defect level fluctuations. The statistics for the 2 fs MD run and their difference from the 10 fs run are presented in Table S2, clearly revealing only small differences in any quantity of interest.

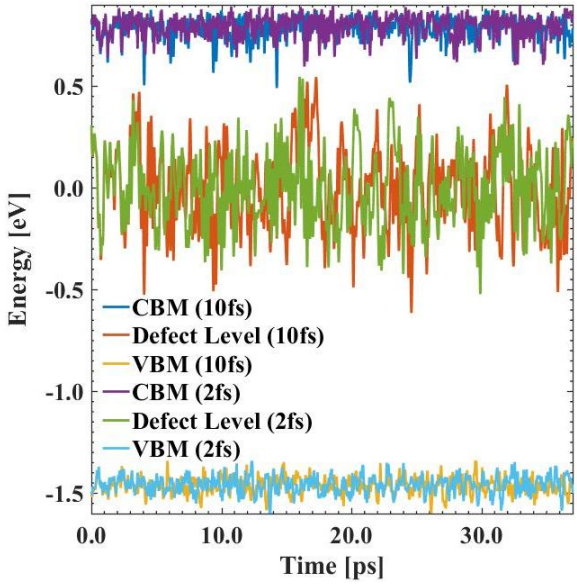

Figure S2: Eigenvalues representing the valence band maximum (VBM), defect level, and conduction band minimum (CBM) as a function of time along the MD trajectory, for a V_{Br}-containing 2x2x2 $CsPbBr_3$ supercell. An MD trajectory with a 2 fs time step is overlaid atop the 10 fs MD trajectory used in the main text.

Table S2: Statistical analysis of the eigenvalues representing the VBM, defect level (E_d), and CBM, performed on the results of the MD run of the V_{Br}-containing $CsPbBr_3$ supercell with a 2 fs time step. The differences from the values received from an MD run with a 10 fs time step of similar duration are given in parenthesis.

	VBM [eV]	**E_d [eV]**	**CBM [eV]**	**CBM-Ed [eV]**
min	0.43 (-0.03)	1.53 (0.08)	2.65 (0.09)	0.27 (0.00)
max	0.71 (-0.01)	2.60 (-0.01)	2.95 (0.01)	1.21 (0.00)
range	0.28 (0.02)	1.07 (-0.09)	0.30 (-0.09)	0.94 (-0.08)
standard deviation	0.04 (0.00)	0.18 (-0.02)	0.05 (0.00)	0.16 (-0.02)
average	0.59 (-0.01)	2.05 (-0.01)	2.85 (0.00)	0.80 (0.00)

Similarly, the same tests conducted for the GaAs system, where the time step was reduced to 1 fs (Fig. S3, Table S3), confirmed that the choice of a 10 fs time step is appropriate.

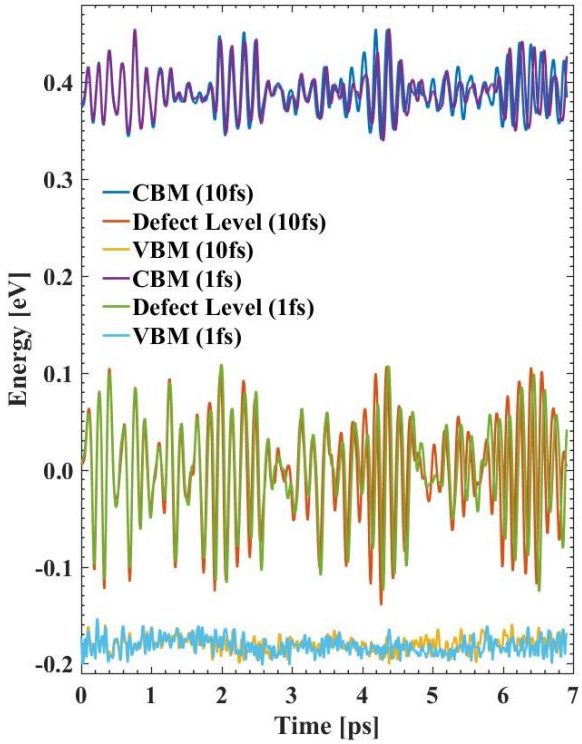

Figure S3: Eigenvalues representing the valence band maximum (VBM), defect level, and conduction band minimum (CBM) as a function of time along the MD trajectory, for a As_{Ga}-containing 3x3x3 GaAs supercell. An MD trajectory with a 1 fs time step is overlaid atop the 10 fs MD trajectory used in the main text.

Table S3: Statistical analysis of the eigenvalues representing the VBM, defect level (E_d), and CBM, performed on the results of the MD run of the As_{Ga}-containing GaAs supercell with a 1 fs time step. The differences from values obtained from an MD run with a 10 fs time step of similar duration are given in parenthesis.

	VBM [eV]	**E_d [eV]**	**CBM [eV]**	**CBM-Ed [eV]**
min	3.99 (0.00)	4.06 (0.01)	4.53 (0.00)	0.32 (0.00)
max	4.03 (0.00)	4.30 (0.00)	4.64 (0.00)	0.49 (0.00)
range	0.05 (0.01)	0.23 (-0.01)	0.12 (0.00)	0.18 (0.00)
standard deviation	0.01 (0.00)	0.05 (0.00)	0.02 (0.00)	0.03 (0.00)
average	4.01 (0.00)	4.19 (0.00)	4.58 (0.00)	0.39 (0.00)

3. k-grid convergence and spin polarization

In this study, we used Γ-point only sampling of the Brillouin zone in order to reduce the computational cost. The HaP band structures in Fig. S4 were obtained using a 2x1x2 k-point sampling and found to be converged numerically. Clearly, also when using this improved setting the main conclusion of the article, i.e., that the defect level position spans a considerable portion of the bandgap, remains unchanged. The spread of the defect energies was found to change by 0.02 eV, which is extremely small compared to the main effect we report. Similarly, in the GaAs system, when comparing the results obtained using Γ-point only sampling to ones obtained using a 2x2x2 k-grid, a difference of 0.03 eV in the spread was found (Table S4).

In a similar vein, the data presented in the main text were obtained using spin-unpolarized calculations. A comparison of Figs. S4(a) and S4(b) shows that the inclusion of spin-polarization in the calculations only increases the range of the defect level energetics (by ~0.2 eV), owing to spin-splitting, thereby only lending further support to our central claims.

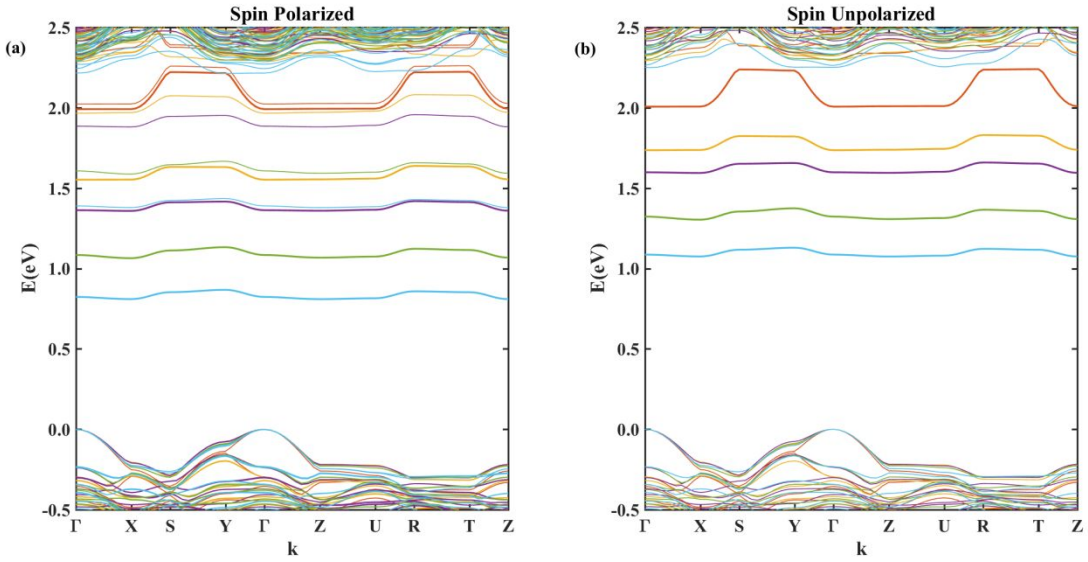

Figure S4: Band structures corresponding to five different geometries sampled from the MD results corresponding to a Br vacancy containing $CsPbBr_3$ supercell, chosen such that the defect level spans the entire range of fluctuations. The band structures are overlaid and presented (a) with and (b) without spin polarization in the calculation. In the former, defect energy levels with similar color correspond to different spin channels of the same state.

Table S4: Statistical analysis of the eigenvalues representing the VBM, defect level (E_d), and CBM, performed on the results of a 15 ps MD run of the As_{Ga}-containing GaAs supercell with 2x2x2 k-grid sampling. The differences from the values received from an MD run with Γ-point only sampling of similar duration are given in parenthesis.

	VBM [eV]	**E_d [eV]**	**CBM [eV]**	**CBM-Ed [eV]**
min	3.97 (0.01)	4.06 (-0.04)	4.51 (-0.01)	0.29 (0.01)
max	4.03 (0.04)	4.30 (-0.01)	4.64 (-0.02)	0.48 (0.04)
range	0.06 (0.02)	0.24 (0.03)	0.13 (-0.01)	0.19 (0.03)
standard deviation	0.01 (0.00)	0.04 (0.00)	0.02 (0.00)	0.03 (0.00)
average	4.00 (0.02)	4.20 (-0.03)	4.56 (0.00)	0.36 (0.03)

4. Convergence with respect to supercell size

Fig. S4 reveals that the shallower the defect level is, the more dispersed it becomes, consistent with the more delocalized nature it adopts. This hints that the 2x2x2 supercell, used in the calculations reported in the main text, may be insufficient for the more delocalized defects. To test this, we "wrapped" the geometry that resulted in the shallowest defect level in Fig. S4 into a bigger supercell, by doubling the length of the *b* axis (the direction of the delocalization). A comparison between the band structures obtained from the two supercells is given in Fig. S5. Clearly, the 2x4x2 supercell is sufficient for containing the delocalized defect, as proven by the "flat" nature of the energy of the defect level. However, the average energy position, and in particular how close the energy is to the band edge, can already be deduced from the smaller supercell, as the energy difference with respect to the conduction band minimum changed by only ~0.1 eV.

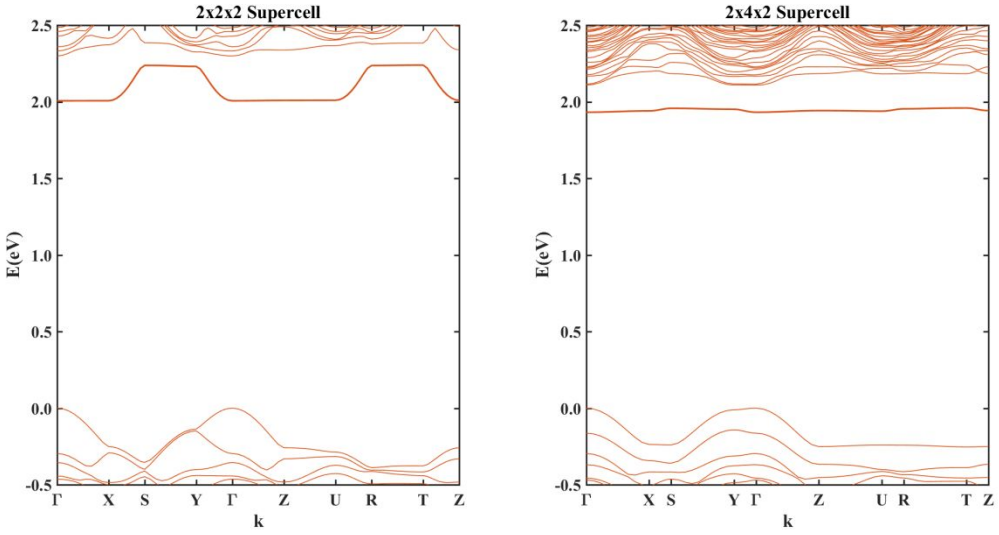

Figure S5: Band structure of a geometry that introduces a defect level close to the conduction band minimum (CBM) in (a) a 2x2x2 and (b) a 2x4x2 supercell.

To further prove that the reported 2x2x2 supercell is sufficiently converged for our purposes, two additional, shorter MD runs were performed, one with a 2x4x2 supercell (11 ps) and one with a 3x3x3 supercell (5 ps). All other parameters remained the same. A comparison of the eigenvalues from each of these shorter MD runs to the eigenvalues obtained from a segment of similar duration of the long, 2x2x2 supercell MD run, is

given in Fig. S6. The statistics obtained from these MD runs and their differences as compared to the MD run of the 2x2x2 supercell are given in Tables S5 and S6. Clearly, the range of defect level fluctuations remains similar to that of the 2x2x2 supercell, and if the statistics are compared between identical durations, then if anything the larger supercells show slightly larger fluctuations of the defect level. This is a direct result of the fact that the defect is mostly contained within the original 2x2x2 supercell and therefore increasing the supercell has a minimal effect on it. In contrast, the fluctuations in the band edges and band gap, which are bulk phenomena, do diminish with an isotropic increase in supercell size, as recently reported by Mayers et al.[3]

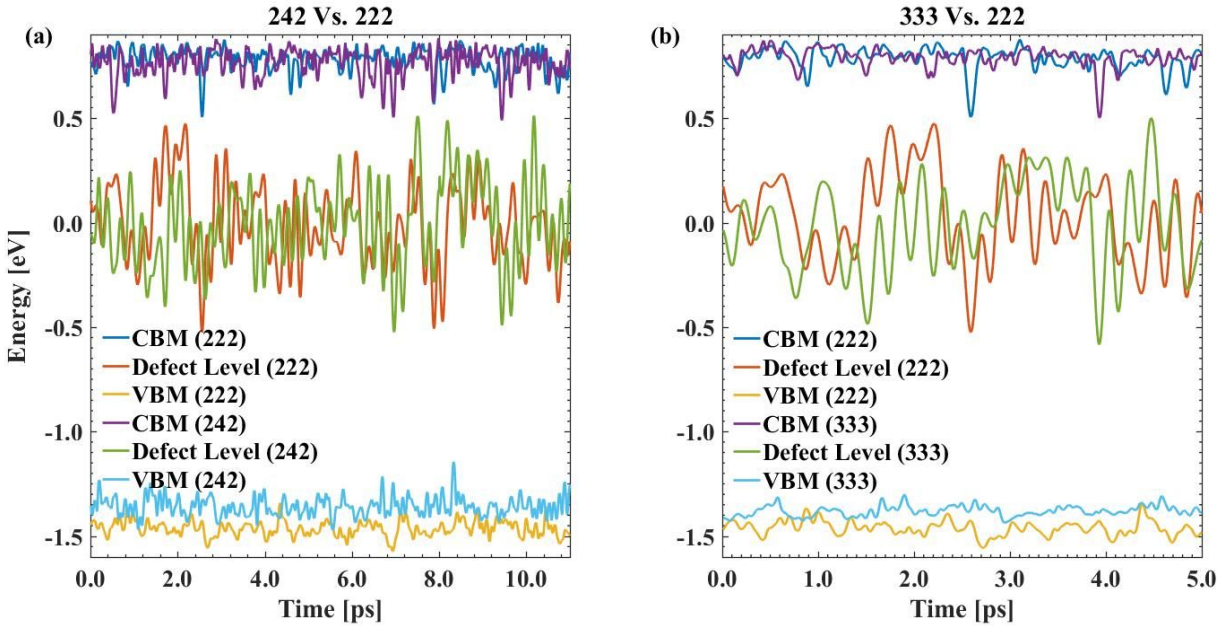

Figure S6: Eigenvalues representing the valence band maximum (VBM), defect level, and conduction band minimum (CBM) as a function of time along the MD trajectory, for a V_{Br}-containing $CsPbBr_3$ (a) 2x2x2 supercell vs. 2x4x2 supercell, (b) 2x2x2 supercell vs. 3x3x3 supercell.

Table S5: Statistical analysis of the eigenvalues representing the VBM, defect level (E_d), and CBM, performed on the results of the MD run of the V_{Br}-containing $CsPbBr_3$ 2x4x2 supercell. The differences from the values obtained from an MD run of a 2x2x2 supercell are given in parenthesis.

	VBM [eV]	**E_d [eV]**	**CBM [eV]**	**CBM-Ed [eV]**
min	0.56 (0.07)	1.51 (-0.03)	2.52 (-0.04)	0.25 (-0.09)
max	0.89 (0.17)	2.54 (0.01)	2.92 (-0.02)	1.13 (-0.01)
range	0.33 (0.09)	1.04 (0.04)	0.39 (0.02)	0.88 (0.08)
standard deviation	0.05 (0.01)	0.19 (-0.01)	0.07 (0.01)	0.17 (0.00)
average	0.68 (0.08)	2.02 (-0.03)	2.79 (-0.05)	0.77 (-0.02)

Table S6: Statistical analysis of the eigenvalues representing the VBM, defect level (E_d), and CBM, performed on the results of the MD run of the V_{Br}-containing $CsPbBr_3$ 3x3x3 supercell. The differences from the values obtained from an MD run of a 2x2x2 supercell are given in parenthesis.

	VBM [eV]	**E_d [eV]**	**CBM [eV]**	**CBM-Ed [eV]**
min	0.62 (0.13)	1.48 (-0.06)	2.56 (-0.01)	0.26 (-0.08)
max	0.76 (0.04)	2.56 (0.02)	2.93 (-0.01)	1.22 (0.09)
range	0.14 (-0.10)	1.08 (0.09)	0.37 (0.00)	0.96 (0.17)
standard deviation	0.02 (-0.01)	0.21 (0.02)	0.05 (-0.01)	0.19 (0.03)
average	0.68 (0.08)	2.05 (-0.01)	2.85 (0.01)	0.80 (0.01)

We performed similar additional MD calculations for the GaAs system, using a 4x4x4 supercell over a 30 ps duration. A comparison of the eigenvalues from this MD run to the eigenvalues obtained from a segment of similar duration of the original, 3x3x3 supercell MD run, is given in Fig. S7. The statistics obtained from the MD run and their differences as compared to the MD run of the 3x3x3 supercell are given in Table S7. Once again, it appears that although overall defect level positions are different, the fluctuations of the defect level are well represented already in the 3x3x3 supercell.

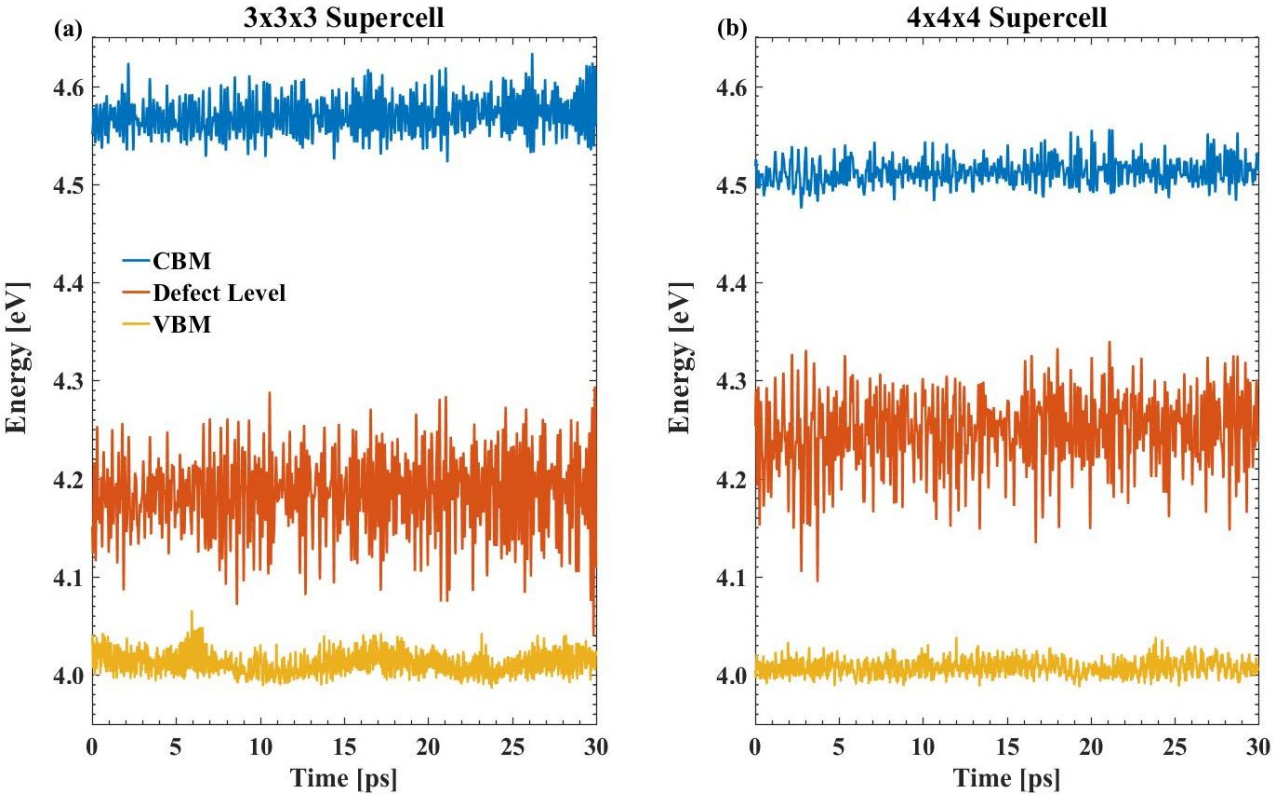

Figure S7: Eigenvalues representing the valence band maximum (VBM), defect level, and conduction band minimum (CBM) as a function of time along the MD trajectory, for a As_{Ga}-containing GaAs (a) 3x3x3 supercell and (b) 4x4x4 supercell.

Table S7: Statistical analysis of the eigenvalues representing the VBM, defect level (E_d), and CBM, performed on the results of the MD run of the As_{Ga}-containing GaAs 4x4x4 supercell. The differences from the values obtained from an MD run of a 3x3x3 supercell are given in parenthesis.

	VBM [eV]	**E_d [eV]**	**CBM [eV]**	**CBM-Ed [eV]**
min	3.99 (0.00)	4.04 (-0.05)	4.52 (0.05)	0.31 (0.11)
max	4.07 (0.03)	4.29 (-0.05)	4.63 (0.08)	0.51 (0.12)
range	0.08 (0.03)	0.25 (0.01)	0.11 (0.03)	0.20 (0.00)
standard deviation	0.01 (0.00)	0.04 (0.00)	0.02 (0.01)	0.03 (0.00)
average	4.01 (0.00)	4.19 (-0.06)	4.57 (0.06)	0.38 (0.12)

5. Defect formation energy and charge transition level theory

In state-of-the art first-principles calculations, the defect formation energy, E^q_{form}, is calculated as:[4]

$$E^q_{form} = E_{defect} - E_{host} - \sum_i n_i\mu_i + q(\varepsilon_F + E_V + \Delta V) + E_{corr} \qquad \text{(S1)}$$

Here, E_{defect} and E_{host} are total energies of the defect-containing and pristine cell, respectively, n_i is the number of atoms of species *i* added or subtracted from the pristine cell, μ_i is the chemical potential, q is the defect charge, ε_F is the Fermi energy position with respect to the valence band maximum (VBM) of the pristine cell (E_V), ΔV is a term that aligns the VBMs of the defect containing and the pristine cell, and E_{corr} is a correction term accounting for remaining spurious electrostatic interaction between the defect and its periodic images. Thermodynamic defect transition levels, which are denoted as $\varepsilon(q_1/q_2)$ and quantify the energy at which one charge state of a specific defect becomes more energetically stable then another one, are then given by:

$$\varepsilon(q_1/q_2) = \frac{E^{q_1}_{form}(\varepsilon_F = 0) - E^{q_2}_{form}(\varepsilon_F = 0)}{q_2 - q_1} \qquad \text{(S2)}$$

In our case, the Br vacancy has two charge states, neutral and positive, and the equation for the transition level can be written as:

$$\varepsilon(0/+1) = E_{defect,\, q=0} - E_{defect,\, q=+1} - (E_V + \Delta V_{q=+1}) + \Delta E_{corr} \qquad \text{(S3)}$$

This equation presents us with a problem when performing an MD analysis, as only one parameter is readily available from the calculation ($E_{defect,\, q=0}$). A partial solution is to take the geometries given by the MD run with the neutral defect and perform a second DFT calculation for each of them with one less electron, thus getting the energy of the positively charged defect ($E_{defect,\, q=+1}$). Note that this method can only provide us with the *vertical* (optical) transition level of the defect, and not the thermodynamic one, which takes into account the different geometries of the different charge states, but that the same limitation applies to defect-related eigenvalues.

We now wish to assess whether defect eigenvalues can indeed act as a reasonable approximation for defect transition levels calculated from Eq. (S3). To that end, we first calculate the transition levels using only the energy difference $E_{defect,\, q=0} -$

$E_{defect,\,q=+1}$, i.e., neglecting the electrostatic and defect-image corrections in Eq. (S3). The results, obtained for the last 15 ps of the MD run, are shown in Fig S8, where they are compared to the defect eigenvalue obtained along the same trajectory. Clearly, the two quantities are strongly correlated throughout (the correlation factor is computed to be 0.98).

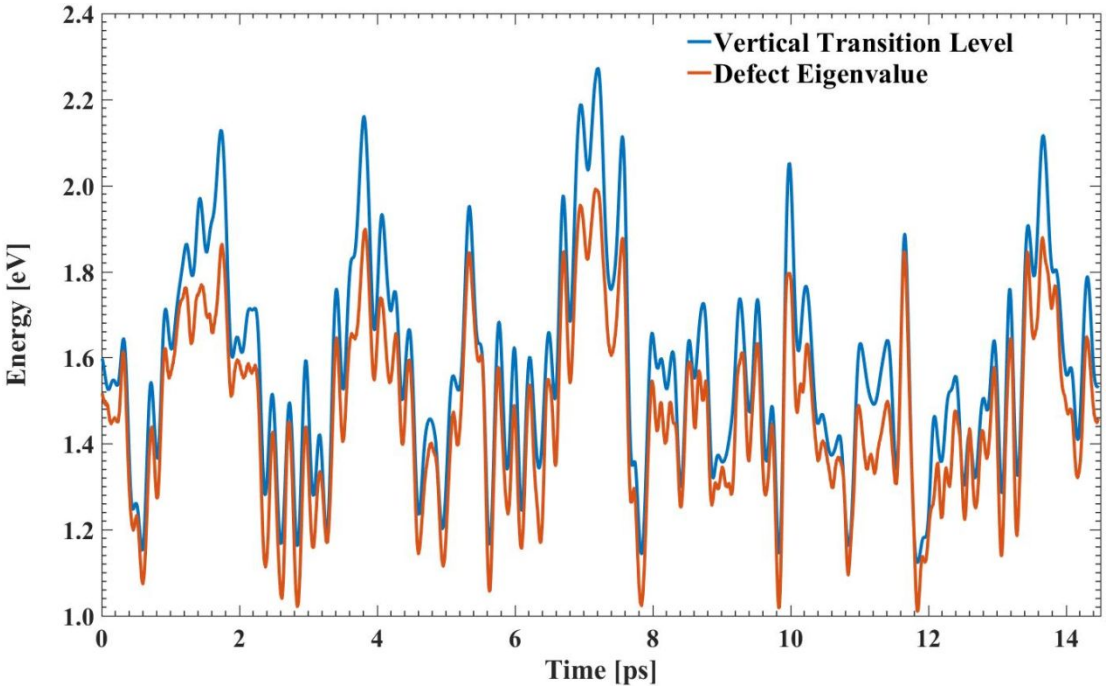

Figure S8: Eigenvalues representing the neutral defect level (orange line), referenced to the valence band maximum (VBM), compared to the vertical transition level of a Br vacancy (taken as the energy difference $E_{defect,\,q=0} - E_{defect,\,q=+1}$, blue line) in a 2x2x2 $CsPbBr_3$ supercell, as a function of time along the MD trajectory for the last 15 ps of run time. This figure has also been given in the main text as Fig. 3 and is shown again here for completeness of the explanation.

We neglect ΔE_{corr} because owing to the super-cell size we don't expect the residual defect-image interactions to be large and therefore to provide a major source of fluctuations in the transition energies. Nevertheless, we are still left with two unknowns in Eq. (S3), $E_V + \Delta V_{q=+1}$, where E_V is the eigenvalue representing the VBM in the pristine material along its MD trajectory and $\Delta V_{q=+1}$ is an alignment term. This alignment term can be found by comparing the energy of a core level (with reference to the electrostatic potential) located far away from the defect, in both the pristine material and the material with the positively charged defect ($\Delta V_{q=+1} = V_{q=+1} - V_{host}$

). The core level energies are readily available from the calculations of the positively charged defect for each MD step ($V_{q=+1}$), but the core level energies of the pristine material (V_{host}) come from a separate MD run with an uncorrelated trajectory. Therefore the two cannot be matched in order to create $\Delta V_{q=+1}$. Similarly, E_V comes from an unrelated trajectory of the host. The fluctuations in the VBM and the Pb 1s core level far from the defect, for the defect-free host material, are given in Fig. S9 and Table S8. While the fluctuations in the VBM are relatively small, the fluctuations in the core level energy are substantial, as the core level energy is a large number to begin with. However, the core level fluctuations for a neutral defect and a positively charged defect, shown in Fig. S10, are almost identical. Clearly, then, for a given geometry, defect energetics have very little effect on the core level position far enough away from the defect. Again, fluctuations in the defect-containing supercell cannot be compared to ones received from the MD run with the pristine material, owing to the different trajectory. However, because electrostatic fluctuations in the defect-free and defect-containing supercell exhibit the same behavior and range of motion, we expect a similar cancellation between core-level fluctuations, i.e., that $\Delta V_{q=+1}$ is small.

Importantly, fluctuations in defect eigenvalue can certainly not be an artefact caused by a change in the electrostatic reference level for each MD step, because then fluctuations in VBM, CBM, and defect level (and for that matter any other eigenvalue) would have to be strongly correlated, as a shift in electrostatic reference shifts all energy levels uniformly. Clearly, this is not the case. Taken together with the high correlation between defect eigenvalues and vertical transition levels established above, defect eigenvalues are indeed a very good approximation for the actual charge transition level.

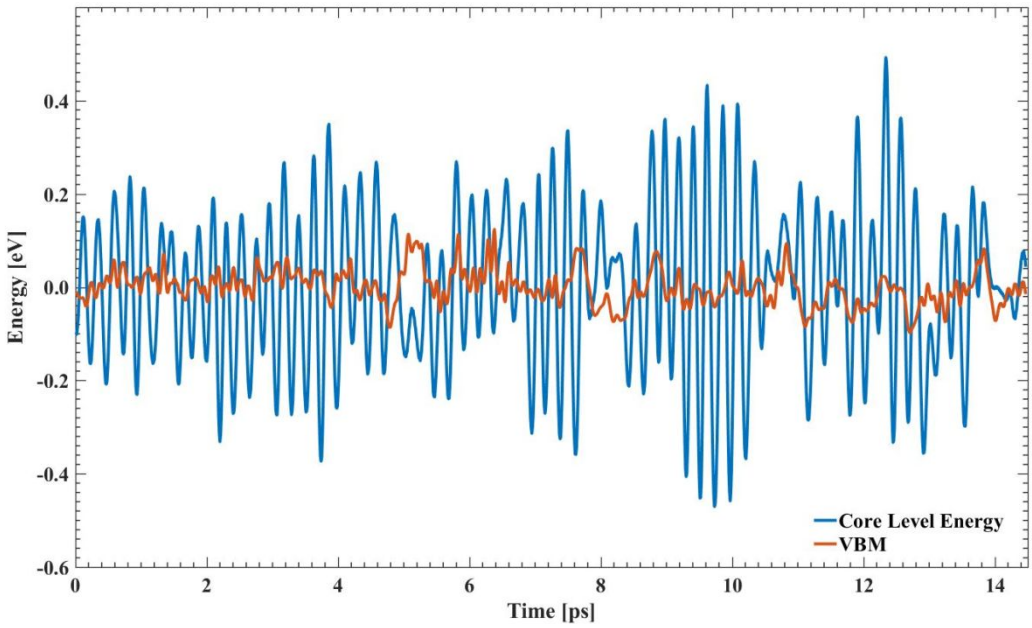

Figure S9: Eigenvalues representing the valence band maximum (VBM) of a pristine 2x2x2 $CsPbBr_3$ supercell along the MD trajectory, as well as the 1*s* core level energy of a Pb atom situated far away from the defect location in a defect-containing cell. All values are referenced to their average along the MD trajectory. Only the last 15 ps of the MD run are shown for ease of viewing.

Table S8: Statistical analysis of the eigenvalues representing the VBM and the 1*s* core level energy of a Pb atom situated far away from the defect location in a defect-containing cell, performed on the results of the MD run of a pristine $CsPbBr_3$ supercell.

	VBM [eV]	Core Level [eV]
Min	0.53	-88085.97
Max	0.77	-88085.01
Range	0.24	0.96
standard deviation	0.03	0.16
Average	0.65	-88085.50

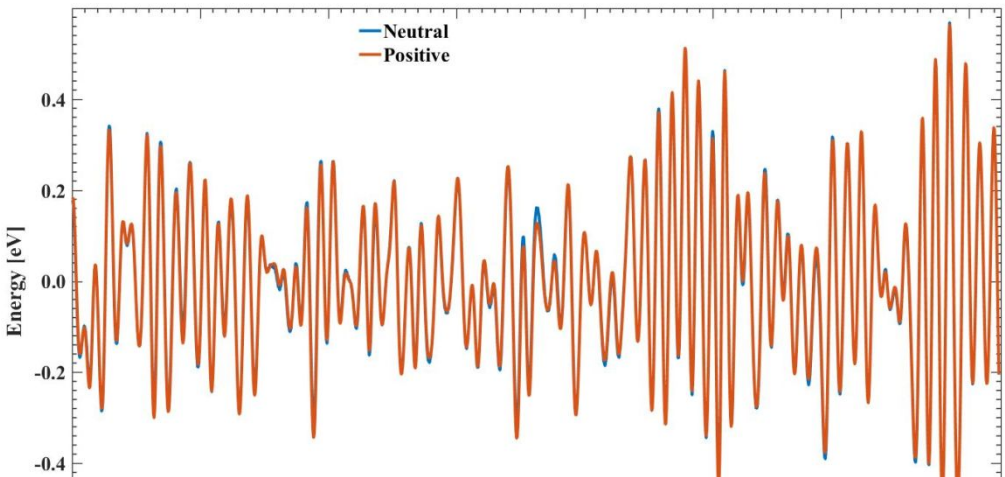

Figure S10: 1*s* core level energies of a Pb atom situated far away from a defect (either neutral or positively charged) location in a defect-containing 2x2x2 $CsPbBr_3$ supercell along the MD trajectory. All values are referenced to their average along the MD trajectory.

6. Correlation coefficients

In the main text, we reported the correlation of the defect level to the conduction band minimum and to the defect's neighboring Pb atoms. In addition, we checked for possible correlation to other neighboring atoms, in terms of both their distance from the defect and the electrostatic potential at their sites. Possible correlation to the VBM, the total energy of the system, and the instantaneous temperature was also checked. All correlation coefficients are presented in Table S9. Clearly, the total energy, the VBM, and the instantaneous temperature are uncorrelated to the defect level fluctuations. The properties of neighboring Cs and Br atoms do have some correlation to the defect level, which is to be expected given that they affect the screening and orbitals of the Pb atoms close to the defect, but this correlation is small compared to that of the neighboring Pb atoms.

Table S9: Correlation coefficients between defect level position and other variables that fluctuate during the MD run.

Parameters correlated to the defect level	**Correlation coefficient**
8 neighboring Br atoms distance from defect	0.00-0.18
4 neighboring Cs atoms distance from defect	0.07-0.14
Electrostatic potential at 8 neighboring Br sites	0.19-0.26
Electrostatic potential at 4 neighboring Cs sites	0.06-0.20
Valence band maximum (VBM)	-0.01
Total energy	0.02
Instantaneous temperature	0.02

7. MD run with a positively charged Br vacancy

We performed an additional MD run with a positively charged Br vacancy. The fluctuations with time of the relevant eigenvalues are given in Fig. S11 and the statistics obtained from the run are presented in Table S10. Clearly, the main conclusions as to the fluctuation of the defect energy level remain the same.

Table S10: Statistical analysis of the eigenvalues representing the VBM, defect level, and CBM, performed on the results of the MD run of $CsPbBr_3$ with a positively charged Br vacancy.

	VBM [eV]	**Defect Level [eV]**	**CBM [eV]**
Minimum	0.53	2.18	2.76
Maximum	0.75	2.91	2.95
Range	0.22	0.73	0.19
Average	0.63	2.70	2.88
Standard Deviation	0.04	0.13	0.03

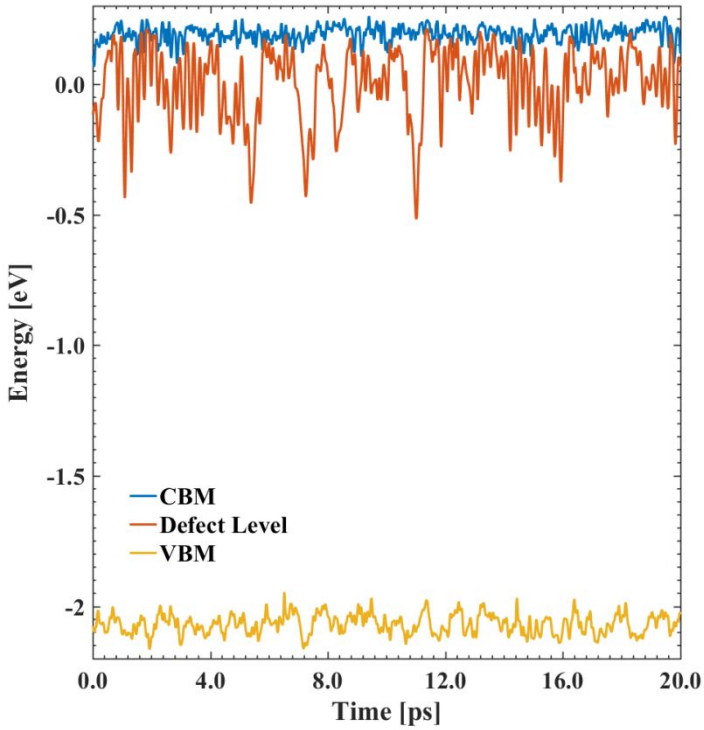

Figure S11: Eigenvalues representing the valence band maximum (VBM), defect level, and conduction band minimum (CBM), as a function of time along the MD trajectory, for $CsPbBr_3$ with a positively charged defect. Only the last 20 ps of the MD run are shown.

References

(1) Heyd, J.; Scuseria, G. E.; Ernzerhof, M. Hybrid Functionals Based on a Screened Coulomb Potential. *J. Chem. Phys.* **2003**, *118* (18), 8207–8215.

(2) Du, M. H. Density Functional Calculations of Native Defects in $CH_3NH_3PbI_3$: Effects of Spin - Orbit Coupling and Self-Interaction Error. *J. Phys. Chem. Lett.* **2015**, *6* (8), 1461–1466.

(3) Mayers, M.; Tan, L. Z.; Egger, D. A.; Rappe, A. M.; Reichman, D. R. How Lattice and Charge Fluctuations Control Carrier Dynamics in Halide Perovskites. *Nano Lett.* **2018**, *18* (12), 8041–8046.

(4) Freysoldt, C.; Grabowski, B.; Hickel, T.; Neugebauer, J.; Kresse, G.; Janotti, A.; Van De Walle, C. G. First-Principles Calculations for Point Defects in Solids. *Rev. Mod. Phys.* **2014**, *86* (1), 253–305.